ERRATUM

Development 136, 1397 (2009) doi:10.1242/dev.036780

Definitive hematopoietic stem/progenitor cells manifest distinct differentiation output in the zebrafish VDA and PBI

Hao Jin, Raman Sood, Jin Xu, Fenghua Zhen, Milton A. English, P. Paul Liu and Zilong Wen

A processing error occurred when the full text HTML for *Development* **136**, 647-654 was produced.

Throughout the full text version the alpha symbol in *αe1-globin* was converted to β, thus in all cases '*βe1-globin*' should read '*αe1-globin*'.

The full text has now been corrected. The PDF and print copy are correct.

We apologise to authors and readers for this mistake.

Development 136, 647-654 (2009) doi:10.1242/dev.029637

Definitive hematopoietic stem/progenitor cells manifest distinct differentiation output in the zebrafish VDA and PBI

Hao Jin[1,*], Raman Sood[2,*], Jin Xu[1], Fenghua Zhen[1], Milton A. English[2], P. Paul Liu[2,†] and Zilong Wen[1,†]

One unique feature of vertebrate definitive hematopoiesis is the ontogenic switching of hematopoietic stem cells from one anatomical compartment or niche to another. In mice, hematopoietic stem cells are believed to originate in the aorta-gonad-mesonephros (AGM), subsequently migrate to the fetal liver (FL) and finally colonize the bone marrow (BM). Yet, the differentiation potential of hematopoietic stem cells within early niches such as the AGM and FL remains incompletely defined. Here, we present in vivo analysis to delineate the differentiation potential of definitive hematopoietic stem/progenitor cells (HSPCs) in the zebrafish AGM and FL analogies, namely the ventral wall of dorsal aorta (VDA) and the posterior blood island (PBI), respectively. Cell fate mapping and analysis of zebrafish *runx1*^{w84x} and *vlad tepes* (*vlt*^{m651}) mutants revealed that HSPCs in the PBI gave rise to both erythroid and myeloid lineages. However, we surprisingly found that HSPCs in the VDA were not quiescent but were uniquely adapted to generate myeloid but not erythroid lineage cells. We further showed that such distinct differentiation output of HSPCs was, at least in part, ascribed to the different micro-environments present in these two niches. Our results highlight the importance of niche in shaping the differentiation output of developing HSPCs.

KEY WORDS: Zebrafish, Hematopoiesis, Ventral wall of dorsal aorta (VDA), Posterior blood island (PBI), Lineage differentiation, Ontogeny

INTRODUCTION

Vertebrate hematopoiesis is characterized by two evolutionarily conserved phases of development: primitive and definitive hematopoiesis (Mikkola and Orkin, 2006; Cumano and Godin, 2007). Primitive hematopoiesis is an early arising but transitory wave, mainly generating primitive erythrocytes and some macrophages. Conversely, definitive hematopoiesis is evoked later and is responsible for the establishment of self-renewable hematopoietic stem cells that are capable of giving rise to all hematopoietic lineages throughout the lifespan of an organism. A shared feature of vertebrate definitive hematopoiesis is the ontogenic switching of hematopoietic stem cells from one anatomical compartment to another (Mikkola and Orkin, 2006; Cumano and Godin, 2007). In mice, hematopoietic stem cells originate in the aorta-gonad-mesonephros (AGM) (Muller et al., 1994; Medvinsky and Dziezak, 1996; Cumano et al., 2001) or perhaps yolk sac (Samokhvalov et al., 2007) and placenta (Gekas et al., 2005; Ottersbach and Dzierzak, 2005), from which they are believed to sequentially colonize fetal liver (FL), the major fetal hematopoietic organ, and bone marrow (BM) in the adult (Mikkola and Orkin, 2006; Cumano and Godin, 2007).

Within these distinct niches, hematopoietic stem cells appear to display niche-specific differentiation repertoire (Mikkola and Orkin, 2006; Cumano and Godin, 2007). In BM, hematopoietic stem cells undergo evident multilineage differentiation through defined intermediates, with progressively restricted self-renewal and differentiation capacity. Common myeloid progenitors and common lymphoid progenitors arguably represent the earliest divergent point of hematopoietic stem cell commitment from which erythro-myeloid and lymphoid cells, respectively, will be derived (Kondo et al., 1997; Akashi et al., 2000). Likewise, in the FL, hematopoietic stem cells proceed to pronounced in situ differentiation into major blood lineages (Cumano and Godin, 2007). However, the differentiation hierarchy of hematopoietic stem cells in the FL probably involves fetal intermediate progenitors that are distinct from those in the BM, as common myeloid progenitors and common lymphoid progenitors isolated from the FL exhibit less strict differentiation potential than do those in BM (Mebius et al., 2001; Traver et al., 2001). In contrast to active multilineage differentiation occurring in the FL and BM, AGM is generally regarded as a site that is devoid of in situ differentiation (Cumano and Godin, 2007). The most compelling evidence to support the differentiation dormancy of hematopoietic stem cells in the AGM comes from in vitro potential assays aimed to detect lineage-restricted progenitors (Godin et al., 1999). These assays fail to find the enrichment of intermediate precursors in the AGM and most hematopoietic cells in this region are multipotent. However, the outcome of such in vitro assays relies heavily on the applied culture condition, which may not faithfully reflect a physiological context. Therefore, an in vivo assay is needed to examine the differentiation capacity of hematopoietic stem cells in the AGM.

By integrating the advantages for both embryological and genetic studies, zebrafish provide unique opportunities to address early development-related biological questions. Similar to higher vertebrates, zebrafish also experience two successive waves of hematopoietic development: primitive and definitive waves (Davidson and Zon, 2004; de Jong and Zon, 2005). Hematopoietic stem cells in zebrafish are thought to arise in the ventral wall of dorsal aorta (VDA), as suggested by their expression of *cmyb* and *runx1* (Thompson et al., 1998; Kalev-Zylinska et al., 2002; Burns et al., 2005; Gering and Patient, 2005) and by in vivo fate mapping (Murayama et al., 2006; Jin et al., 2007; Kissa et al., 2008). We have termed these presumed zebrafish definitive hematopoietic stem cells as definitive hematopoietic stem/progenitor cells (HSPCs), acknowledging that supporting

[1]Department of Biochemistry, the Hong Kong University of Science and Technology, Clear Water Bay, Kowloon, P. R. China. [2]National Human Genome Research Institute, National Institutes of Health, Building 49, Room 3A26, Bethesda, MD 20892, USA.

*These authors contributed equally to this work
†Authors for correspondence (e-mail: pliu@nhgri.nih.gov; zilong@ust.hk)

Accepted 15 December 2008

functional data are still lacking. These VDA-originating HSPCs are subsequently mobilized to an intermediate compartment, the posterior blood island (PBI) or caudal hematopoietic tissue (CHT), prior to their final colonization of the adult hematopoietic organ, the kidney (Murayama et al., 2006; Jin et al., 2007). Thus, functional analogies of AGM and FL in zebrafish are very likely to be represented by the VDA and PBI, respectively. However, to date, the differentiation profile of HSPCs within the VDA and PBI is still poorly defined.

Here, we presented an in vivo cell fate analysis in zebrafish embryos to explore the lineage differentiation repertoire of HSPCs in the VDA and PBI, with particular focus on their differentiation into erythroid and myeloid lineages. We found that HSPCs were incapable of giving rise to erythroid lineage in the VDA until they migrated to the PBI. However, to our surprise, despite the inability of HSPCs to produce erythroid cells in the VDA, in situ differentiation into myeloid lineages was readily detected in this region, indicating that HSPCs in the AGM are not quiescent with respect to their differentiation. We further showed that HSPCs lost the ability to give rise to erythroid lineages when forced to remain in the VDA, suggesting that selective emergence of definitive erythropoiesis in the PBI is at least partly due to distinct micro-environment in the VDA and PBI.

MATERIALS AND METHODS

Maintenance of fish strains

Zebrafish were bred as described (Westerfield, 1995). The following fish strains were used: AB, Tg(*fli1*:eGFP) (Lawson and Weinstein, 2002) and *vlad tepes* (*vlt*^{m651}) (Lyons et al., 2002). The *runx1*^{W84X} mutation was identified from F1 fish of ENU-treated founders through genomic PCR and sequencing. The genomic organization of zebrafish *runx1* was determined using NCBI and Sanger Center databases. Sequencing of exons of interest, data analysis and in vitro fertilization to recover the mutation were performed as described previously (Sood et al., 2006).

Laser activated cell labeling

Lineage tracking was adapted from a compilation of previous publications (Vincent and O'Farrell, 1992; Kozlowski et al., 1997; Melby et al., 1996; Serbedzija et al., 1998; Keegan et al., 2004). Our modified procedure has been described by Jin et al. (Jin et al., 2007).

In vitro synthesis of antisense RNA probe

Antisense RNA probes were prepared by in vitro transcription according to standard protocol (Westerfield, 1995). The following probes were used in the study: digoxigenin (DIG)-labeled antisense *αe1-globin* (*hbae1* – Zebrafish Information Network), *lyc* (*lyz* - Zebrafish Information Network), *mpo* (*mpx* – Zebrafish Information Network), *l-plastin* (*lcp1* – Zebrafish Information Network), *cmyb* and *runx1* probes.

Single-color whole-mount in situ hybridization

Single-color whole-mount in situ hybridization was performed as described previously (Westerfield, 1995).

Two color fluorescence in situ hybridization

To detect uncaged fluorescein (flu) and *lyc* transcript or flu and *αe1-globin* transcript simultaneously, embryos were first hybridized with DIG-labeled antisense RNA probe at 68°C overnight. After washing and blocking, embryos were incubated at 4°C overnight with POD-conjugated anti-flu antibody (1:500) (Roche) and stained with Alexa Fluor 488 tyramide substrate (Molecular Probes) according to manufacturer's instructions. The color reaction was then stopped by sequentially washing with 25%, 50% and 75% methanol/PBST (10 minutes); 1% H_2O_2/methanol (30 minutes); 75%, 50% and 25% methanol/PBST (10 minutes); PBST (2×5 minutes). Finally, embryos were subjected to second color staining with anti-DIG POD (1:1000) (Roche) and Alexa Fluor 555 tyramide as substrate (Molecular Probes).

Double fluorescence antibody staining

Immunohistochemistry was performed essentially as described previously (Jin et al., 2006). To examine the co-staining of flu and L-plastin, flu was stained by anti-flu-POD (1:500, 4°C, overnight) with Alexa Fluor 555 as substrate. The rabbit anti-zebrafish L-plastin antibody was generated with glutathione-S-transferase-L-plastin (amino acids 9 to 149) fusion protein and used at 1:300 dilution. Anti-L-plastin antibody was further visualized by Alexa Fluor 647 donkey anti-rabbit (1:400, 4°C, overnight) (Molecular Probes).

Double staining for *cmyb* RNA and L-plastin protein

Staining for *cmyb* RNA was first developed with Alexa Fluor 555 tyramide. Afterwards, embryos were washed with PBST for 6×20 minutes at room temperature before proceeding to antibody staining for zebrafish L-plastin. Embryos were incubated with anti-L-plastin antibody (1:300 dilution, 4°C, overnight) and visualized by Alexa Fluor 488 donkey anti-rabbit (1:400, 4°C overnight) (Molecular Probes).

Morpholino injection

runx1 MO-1 (5′-TGTTAAACTCACGTCGTGGCTCTC-3′) and *runx1* MO-2 (5′-AATGTGTAAACTCACAGTGTAAAGC-3′) were designed based on the sequence published by Burns et al. (Burns et al., 2005). One-cell stage embryos were injected with 2 nl morpholino solution at a concentration of 0.6 mM *runx1* MO-1 and 1 mM *runx1* MO-2. The *silent heart* MO was designed and injected according to a previous report (Sehnert et al., 2002). A standard control MO was obtained from Gene Tools.

May-Grunwald Giemsa staining

May-Grunwald Giemsa (Sigma) staining was performed as described previously (Qian et al., 2007).

RESULTS

Definitive erythrocytes are enriched in the PBI from 3.5 dpf onwards

To define the onset of definitive erythropoiesis, we first mapped the temporal-spatial development of *αe1-globin* RNA-expressing cells with whole-mount in situ hybridization. As *αe1-globin* RNA expression was reported to be reactivated during later stages of development (Brownlie et al., 2003), detailed analysis of expression pattern of *αe1-globin* transcript might aid in revealing the initiation of definitive erythropoiesis. Consistent with a previous report (Brownlie et al., 2003), we observed that the number of *αe1-globin* transcript-positive cells peaked at around 2 days post-fertilization (dpf) and subsequently declined to a few cells by 3 dpf (Fig. 1B,C). Such declination from 2 dpf to 3 dpf reflects the cessation of *αe1-globin* transcription in primitive erythrocytes. However, *αe1-globin* RNA-expressing cells increased in number when embryos reached 3.5-4.0 dpf (Fig. 1D). The propagation of these cells appeared to be confined to the PBI, with their particular absence in the VDA (Fig. 1D). By 5 dpf, the *αe1-globin* RNA-expressing cells were also seen in the kidney (Fig. 1E, arrow). This late arising population of *αe1-globin* transcript-positive cells probably represents newly generated cells of definitive erythroid lineage, as their appearance temporally correlated with the emergence of circulating erythroid precursors with a morphological characteristic similar to the definitive proerythroblasts found in the adult kidney (Traver et al., 2003) (see Fig. S1 in the supplementary material). To illustrate convincingly the definitive origin of these PBI restricted *αe1-globin* RNA-positive cells, we probed *αe1-globin* transcript in embryos in which definitive hematopoiesis was inhibited by either *runx1* antisense morpholino oligonucleotide (MO) or a *runx1* mutation in the *runx1*^{w84x} mutants. *runx1*^{w84x} was isolated by screening exons 3 and 4 of zebrafish *runx1* gene through genomic PCR and sequencing (Sood et al., 2006). It harbors a G to A nucleotide substitution that converts a Trp (amino acid 84) encoding triplet (UGG) to a

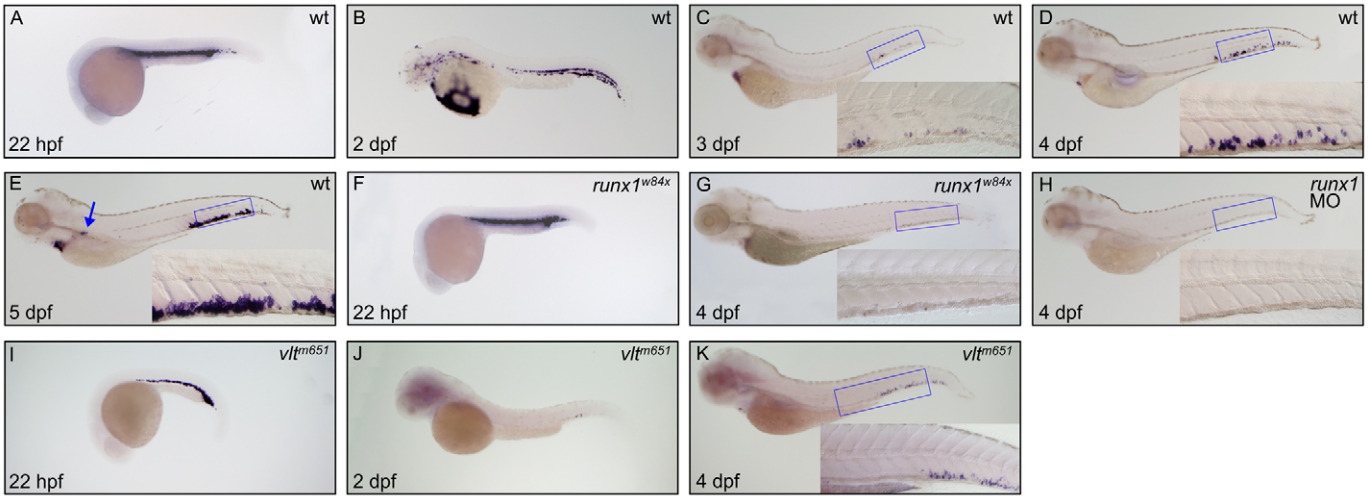

Fig. 1. Definitive erythroid cells arise in the PBI but not the VDA. (**A-K**) Whole-mount in situ hybridization to detect αe1-globin expression in wild-type embryos (A-E) at 22 hpf (A), 2 dpf (B), 3 dpf (C), 4 dpf (D) and 5 dpf (E); *runx1*^{w84x} mutant (F,G) and morphant (H) embryos at 22 hpf (F) and 4 dpf (G,H); and *vlt*^{m651} embryos (I-K) at 22 hpf (I), 2 dpf (J) and 4 dpf (K). The blue arrow in E indicates αe1-globin expression in pronephros. The insets are higher magnification (20×) views of the corresponding boxed regions (blue).

premature stop codon (UGA) (see Fig. S2A in the supplementary material). The resulting truncated protein lacks majority of the Runt domain and therefore could be considered as null. It is known that suppression of *runx1* gene expression will specifically abolish the formation of definitive HSPC and its derivatives without affecting primitive hematopoiesis (Okuda et al., 1996; Burns et al., 2005; Gering and Patient, 2005). In line with this, we found that in the *runx1* morphants and homozygous *runx1*^{w84x} mutants, *cmyb*-positive definitive hematopoietic progenitors, including HSPCs, were absent from all definitive hematopoietic tissues, including VDA, PBI and kidney (see Fig. S2B-E in the supplementary material). Moreover, we observed that primitive erythroid cells in the intermediate cell mass (ICM) were not perturbed in *runx1*^{w84x} mutants (compare Fig. 1F with 1A) and *runx1* MO knockdown embryos (morphants) (data not shown). By contrast, *αe1-globin* RNA-positive cells in the PBI and circulating definitive proerythroblasts were absent in *runx1*^{w84x} mutants (Fig. 1G) and *runx1* morphants (Fig. 1H) (n=46/52) (see Fig. S1C in the supplementary material), showing that these cells are indeed of definitive origin.

Definitive erythropoiesis initiates from the PBI but not VDA

The enrichment of definitive erythroid cells in the PBI suggests that the onset of definitive erythropoiesis in zebrafish occurs in the PBI rather than the VDA. However, it could be conceived that abundant production of definitive erythrocytes in the PBI is the consequence of the migration, proliferation and differentiation of a small population of committed definitive erythroid progenitors specified earlier in the VDA. This small cell population could be masked by the presence of numerous primitive erythrocytes in wild-type embryos. To clarify this possibility, we examined the expression profile of *αe1-globin* transcript in the *vlad tepes* (*vlt*^{m651}) mutants, which harbor a nonsense mutation in the essential erythroid regulator *gata1* (Lyons et al., 2002). In *vlt*^{m651}, primitive erythroid progenitors are specified normally but subsequently depleted by 48 hpf, owing to accelerated apoptosis (Lyons et al., 2002). As one would anticipate that *gata1* exerts similar functions during definitive erythropoiesis, the *vlt*^{m651} mutants could be used to observe the emergence of the earliest committed definitive erythroid progenitors, without the interference of primitive erythrocytes. As shown in Fig. 1I,J, the number of *αe1-globin* RNA-positive cells in *vlt*^{m651} embryos drastically reduced from a large number at 22 hpf to only a few cells at 48 hpf. These rare cells in the 48 hpf *vlt*^{m651} embryos were randomly distributed, indicating that they were just vestige of primitive erythrocytes. Hence, it is reasonable to believe that the reappearance of *αe1-globin* transcription after 48 hpf is a sign of the committed definitive erythroid progenitors. As shown in Fig. 1, albeit the magnitude is low in *vlt*^{m651} embryos compared with wild-type siblings, the number of *αe1-globin* transcript-positive cells indeed increased from 3 dpf onwards and reached its peak by 4 dpf (Fig. 1K). More importantly, these newly emerged definitive erythroid progenitors were first evident in the PBI rather than VDA (Fig. 1K), indicating that the commitment to definitive erythroid lineage took place in the PBI. As expected, these PBI restricted *αe1-globin* mRNA-positive cells in *vlt*^{m651} significantly diminished from 5 dpf onwards (data not shown), reflecting similar requirement of *gata1* during maturation of definitive erythroid lineage. Taken together, the analysis of erythroid development in both wild-type and *vlt*^{m651}embryos clearly support the argument that the initiation of definitive erythropoiesis occurs in the PBI but not in the VDA.

To determine whether PBI HSPCs that gave rise to definitive erythropoiesis were originated from the VDA, we used a photo activatable cell tracer, 4,5-dimethoxy-2-nitrobenzyl (DMNB) caged fluorescein (flu), to label HSPCs in the VDA, in order that their fates could be followed subsequently (Vincent and O'Farrell, 1992; Kozlowski et al., 1997; Melby et al., 1996; Serbedzija et al., 1998; Keegan et al., 2004; Jin et al., 2007). DMNB caged flu was injected into one-cell stage Tg(*fli1*:eGFP) embryos in which HSPCs were also marked by GFP (Jin et al., 2007; Lawson and Weinstein, 2002). At 30 hpf, a small population (two or three) of GFP-positive cells in the anterior part of VDA was uncaged with 405 nm laser (Fig. 2A), and contribution of these flu-labeled cells to definitive erythrocytes was examined by co-staining of flu and *αe1-globin* RNA at 4 dpf (Fig. 2B-F). We observed that nine out of 28 uncaged embryos contained flu/*αe1-globin* co-stained cells (Fig. 2C-F). Remarkably,

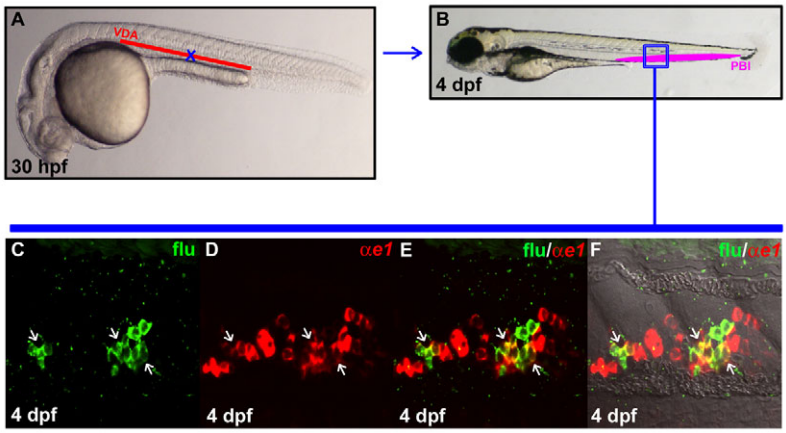

Fig. 2. VDA originated HSPCs are capable of giving rise to definitive erythroid cells once homed to the PBI. (**A**) Lateral view of 30 hpf embryo indicates the uncaged position (blue cross) in the anterior part of VDA. (**B**) Lateral view of 4 dpf embryo. The boxed region (blue) indicates the relative position in the PBI where flu and *αe1-globin* RNA double-positive cells are found after uncaging. (**C**,**D**) Confocal images of the boxed region in B show the flu signal and *αe1-globin* RNA staining in the PBI. (**E**) Merged image of C and D. (**F**) Superimposed view of E and DIC image. White arrows indicate the co-staining of flu and *αe1-globin* RNA.

these flu/*αe1-globin* double-positive cells were exclusively located in the PBI, confirming that HSPCs originated from the VDA are capable of differentiating into erythroid cells only when they reach the PBI region. Collectively, these data demonstrate that in the VDA HSPCs are inactive with respect to their commitment and differentiation into definitive erythroid lineage; this activity is later revived upon their homing to the PBI.

Definitive myeloid cells emerge in both the VDA and PBI

Because of the closely related ontogenic development of myeloid and erythroid lineages during the adult phase of definitive hematopoiesis (Akashi et al., 2000), we next asked whether definitive myelopoiesis shared similar features to definitive erythropoiesis during the early phase of zebrafish definitive hematopoiesis, i.e. whether definitive myelopoiesis was also inactive in the VDA but became activated in the PBI. To shed light on this, we examined the distribution of myeloid cells using whole-mount in situ hybridization with differentiated myeloid-specific markers, such as *lyc*, *mpo* and *l-plastin* during zebrafish development (Herbomel et al., 1999; Bennett et al., 2001; Liu and Wen, 2002). An intriguing aspect of myeloid cell development was revealed. At an earlier developmental stage, 22 hpf, myeloid cells were restricted to the rostral part of the embryo, mainly scattered on the yolk sac (data not shown). These cells are known to represent primitive myeloid cells derived from the rostral blood island (RBI) (Herbomel et al., 1999; Lieschke et al., 2002). As embryos developed, myeloid cells gradually emerged in the posterior part of embryo with particular enrichment in the PBI and the region surrounding the VDA (Fig. 3C,E,G; see Fig. S3B,C,H,I in the supplementary material). The close proximity of myeloid cells and HSPCs in the VDA raised an interesting possibility that these myeloid cells were of definitive origin and derived from in situ differentiation of HSPCs. To prove definitive hematopoietic origin of these myeloid cells, we analyzed myeloid cell development in embryos with compromised definitive hematopoiesis through repression of *runx1* gene expression. Largely in accordance with the dispensable role of *runx1* in primitive hematopoietic lineage development, we found that the expression of *l-plastin* remained unaffected in *runx1*^{w84x} mutant (compare Fig. 3B with 3A) and *runx1* morphants at 24 hpf (data not shown). Similarly, the expression of *lyc* and *mpo* was not altered in *runx1* morphants (data not shown) but was slightly decreased in *runx1*^{w84x} mutants (see Fig. S3A,D,G,J in the supplementary material). Contrary to largely intact primitive myeloid program in *runx1*-depleted embryos, the number of myeloid cells in both the VDA and the PBI dramatically decreased in 2 dpf *runx1*^{w84x} mutants (Fig. 3D) and *runx1* morphants (data not shown, *n*=42/50), as well as 3 dpf *runx1*^{w84x} mutants (Fig. 3F; see Fig. S3E,K in the supplementary material). In fact, virtually no myeloid cells were detected in VDA and PBI of the 5 dpf *runx1*^{w84x} mutants (Fig. 3H; see Fig. S3F,L in the supplementary material) and *runx1* morphants (data not shown, *n*=36/42). Thus, the disappearance of myeloid cells in the VDA and PBI in the *runx1*-suppressed embryos indicates that most if not all of this cell population belong to definitive hematopoietic lineages.

Myeloid cells in the VDA are generated via in situ differentiation of HSPCs

To confirm that HSPCs in the VDA could give rise to myeloid cells locally, two or three GFP-positive cells in the anterior part of VDA of Tg(*fli1*:eGFP) embryos were uncaged at 30 hpf and contribution of these flu-labeled cells to myeloid lineage was examined by co-

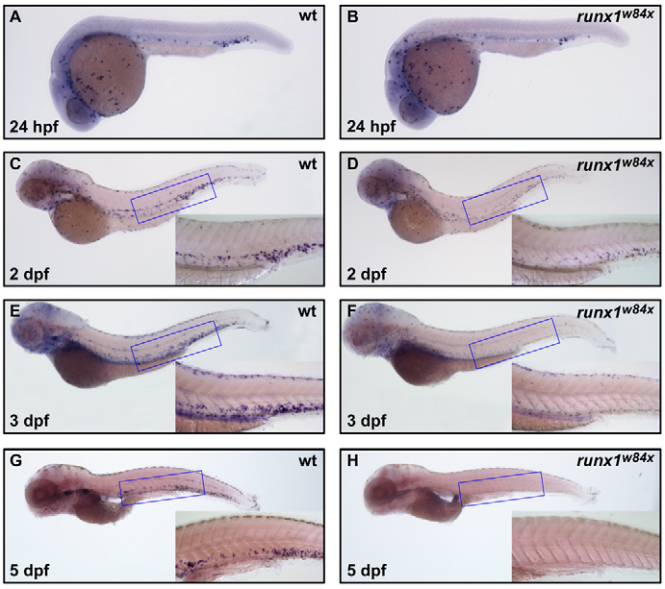

Fig. 3. Enrichment of definitive myeloid cells in the VDA and the PBI. (**A-H**) Whole-mount in situ hybridization of l-plastin expression in wild-type embryos at 24 hpf (A), 2 dpf (C), 3 dpf (E) and 5 dpf (G), and *runx1*^{w84x} mutant embryos at 24 hpf (B), 2 dpf (D), 3 dpf (F) and 5 dpf (H). Insets are high magnification (20X) of the corresponding boxed regions (blue).

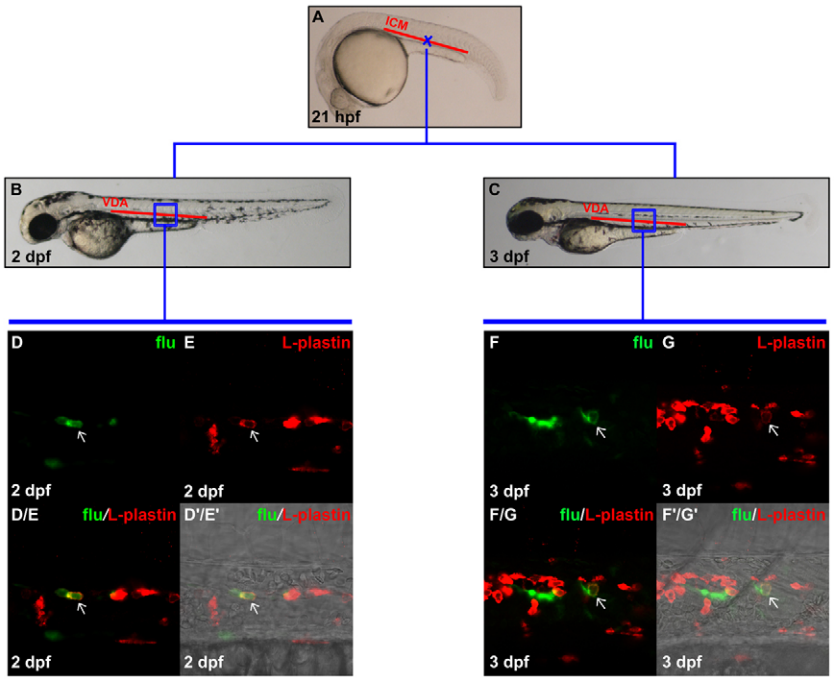

Fig. 4. Definitive myeloid cells are generated in the VDA. (**A**) Lateral view of 21 hpf embryo, indicating the uncaging position (blue cross) in the anterior part of the ICM. (**B**,**C**) Lateral view of 2 dpf (B) and 3 dpf (C) embryos. The boxed regions indicate the relative positions in the VDA where flu and L-plastin protein double-positive cells were detected after uncaging. (**D**,**E**) Confocal images of the boxed region in B showing the flu signal and L-plastin staining in the VDA at 2 dpf after uncaging at cross in A. (**D/E**) Merged image of D and E. (**D′/E′**) Superimposed view of D/E and DIC image. (**F**,**G**) Confocal images of the boxed region in C showing the flu signal and L-plastin staining in the VDA at 3 dpf after uncaging at cross in A. (**F/G**) Merged image of F and G. (**F′/G′**) Superimposed view of F/G and DIC image. Staining for flu and L-plastin is pseudopainted as green and red, respectively. Arrows indicate co-staining of flu and L-plastin.

staining of flu and L-plastin at 3 dpf. We observed that six out of 14 uncaged embryos contained flu/L-plastin double-positive cells in the uncaged region (data not shown), suggesting that the VDA was capable of generating myeloid cells. To avoid inadvertently labeling myeloid cells originated from RBI and unambiguously proving that these VDA-restricted myeloid cells were indeed generated within the VDA region via in situ differentiation of HSPCs, rather than seeded from other hematopoietic sites, we labeled HSPCs at 21 hpf, before circulation started and before primitive myeloid cells migrated to the trunk region (Herbomel et al., 1999; Bennett et al., 2001; Lieschke et al., 2002; Liu and Wen, 2002). At 21 hpf, HSPCs capable of giving rise to T cells are localized to intermediate cell mass (ICM), a precursor to the VDA (Jin et al., 2007). Two or three cells in the anterior ICM of 21 hpf Tg(*fli1*:eGFP) embryos were uncaged (Fig. 4A; see Fig. S4A in the supplementary material), and differentiation of these labeled cells into myeloid cells was determined with double staining against flu and L-plastin protein or *lyc* RNA at 2 dpf or 3 dpf (Fig. 4B-F′/G′; see Fig. S4B-J in the supplementary material). In 24 uncaged embryos that survived to 2 dpf, seven contained flu/L-plastin co-stained cells in the uncaged area (four exclusively in the uncaged area and the other three in both uncaged and PBI region) and one embryo contained flu/L-plastin double positive cells only in the PBI region (Fig. 4B,D-D′/E′; Table 1). The average number of flu/L-plastin co-staining cells in each of these embryos was 2-3. Likewise, when uncaged embryos were examined for myeloid contribution at 3 dpf, nine out of 25 uncaged embryos had flu labeled cells contributed to L-plastin$^+$ myeloid cells in the original uncaged region (five exclusively in the uncaged area and the other four in both uncaged and PBI region) and two embryos were found to harbor flu/L-plastin double-positive cells only in the PBI (Fig. 4C,F-F′/G′; Table 1). Similar results were obtained by detecting co-localization of flu and *lyc* RNA (see Fig. S4 in the supplementary material; Table 1). Thus, as opposed to the apparent absence of definitive erythropoiesis in the VDA, these in vivo tracing experiments demonstrate that definitive myeloid cells do arise in the VDA via in situ differentiation of HSPCs.

Extrinsic factors are essential in determining differentiation output of HSPCs

The abovementioned lineage analysis clearly documents that HSPCs in the VDA differ in their differentiation output from those in the PBI. Although HSPCs give rise to only myeloid cells in the VDA, both erythroid and myeloid cells are produced in the PBI. To explore the underlying basis for distinct lineage output of HSPCs within different compartments, we therefore asked whether such difference was solely controlled by a program intrinsic to HSPCs or whether the micro-environment substantially contributed to this process. To shed light on this, we scrutinized the expression of *cmyb*, a marker for early definitive hematopoietic progenitors, including HSPCs, at 4 dpf, which is when definitive erythrocytes have emerged in PBI.

Table 1. Autonomous production of definitive myeloid cells in the VDA

Genetic background	Marker	Uncaging position	Stage examined	Co-stained cells in the uncaged region	Co-stained cells in the PBI
Wild type	L-plastin	Anterior ICM	2 dpf	7/24*	4/24*
			3 dpf	9/25†	6/25†
	lyc	Anterior ICM	2 dpf	7/22‡	3/22‡

The ratio indicates the number of embryos containing flu/myeloid marker co-stained cells in the corresponding region versus total number of uncaged embryos.
*Three embryos contain co-stained cells in both uncaged region and PBI.
†Four embryos contain co-stained cells in both uncaged region and PBI.
‡Two embryos contain co-stained cells in both uncaged region and PBI.

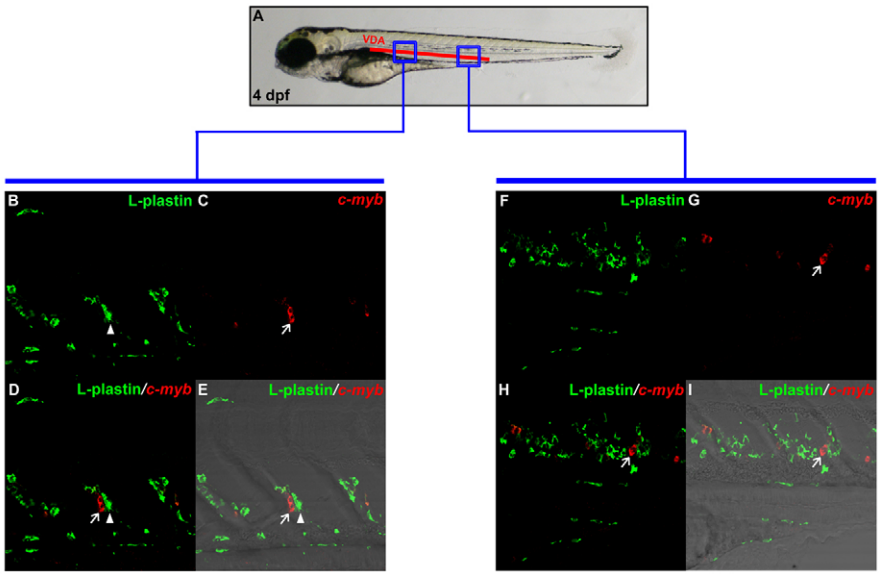

Fig. 5. HSPCs are found in the VDA in 4 dpf wild-type embryos. (**A**) Schematic illustration of 4 dpf embryo, indicating blue boxed regions that are magnified in B-E and F-I. (**B**,**C**) Double staining of L-plastin protein (B) and *cmyb* RNA (C) in anterior VDA portion of 4 dpf wild-type embryo. (**D**) Superimposed image of B and C. (**E**) Merged view of D with DIC image. (**F**,**G**) Double staining of L-plastin protein (F) and *cmyb* RNA (G) in posterior VDA region of 4 dpf wild-type embryo. (**H**) Superimposed image of F and G. (**I**) Merged view of H with DIC image. Arrows indicate HSPCs that are *cmyb*-positive only, whereas arrowheads represent L-plastin-positive myeloid cells.

We noted that, in addition to the PBI, presumptive HSPCs expressing *cmyb* but not the differentiation markers *l-plastin* (Fig. 5A-I) and *αe1-globin* (Fig. 1D,K) were present in the VDA at 4 dpf. Unlike their counterparts in the PBI, these VDA-localized HSPCs did not give rise to definitive erythroid lineages (Fig. 1D,K). The co-existence of definitive erythrocytes and HSPCs in the PBI but not in the VDA at 4 dpf indicates that the PBI micro-environment may play a crucial role in initiating definitive erythropoiesis.

To further substantiate the role of PBI in triggering definitive erythropoiesis, we analyzed erythroid development in the *sih* (silent heart) morphants, in which circulation was blocked by MO-mediated inhibition of cardiac troponin T, thereby forcing HSPCs to remain in the VDA (Sehnert et al., 2002; Murayama et al., 2006). To avoid interference from primitive erythropoiesis, *sih* MO was injected into *vlt*^{m651} embryos, in which primitive erythrocytes were depleted without perturbation of early specification of definitive erythroid progenitors. Consistent with previously reported experiments performed in wild-type embryos (Murayama et al., 2006), the initiation of HSPCs in the VDA was not affected in the *sih* MO-injected *vlt*^{m651} embryos, as detected by *runx1*$^{+}$/*c-myb*$^{+}$ cells at 30 hpf (Fig. 6A-D). HSPCs began to accumulate in the VDA of *sih* MO-injected *vlt*^{m651} embryos by 2 dpf (data not shown) and this accumulation became more evident at 3 dpf (Fig. 6F). In 4 dpf *sih* MO-injected *vlt*^{m651} embryos, these HSPCs largely remained at the VDA, and were hardly detectable at the PBI (Fig. 6H) (n=28/30). Of note, the number of *cmyb*-positive HSPCs in 3 dpf and 4 dpf *sih* MO-injected *vlt*^{m651} embryos appeared comparable with that in the controls (Fig. 6E-H), indicating normal progression of HSPC development. When erythroid development was analyzed, *αe1-globin* mRNA-positive definitive erythroid progenitors emerged normally in the PBI of 4 dpf control MO injected *vlt*^{m651} embryos (Fig. 6I). However, in the *sih* MO-injected *vlt*^{m651} embryos, these definitive erythroid progenitors were not detected either in the PBI or the VDA where HSPCs were located (Fig. 6J) (n=42/45). To demonstrate that the HSPCs trapped in the VDA were still capable of definitive hematopoiesis, in situ hybridization for *lyc* was performed in 4 dpf *sih* MO-injected *vlt*^{m651} embryos, in order to detect definitive myeloid cells. As can be seen in Fig. 6K,L, *lyc*+ myeloid cells were readily detected, which were preferentially localized to the VDA. Taken together, the data strongly suggest that homing to PBI facilitates definitive erythropoiesis. Intriguingly, some myeloid cells were still detectable in the PBI of *sih* MO-injected *vlt*^{m651} embryos. This could result from circulation-independent migration of myeloid cells or from in situ differentiation of committed erythroid/myeloid progenitors originated from the caudal part of precirulation embryos (Bertrand et al., 2007).

DISCUSSION

In the present study, we focused on the characterization of the in vivo differentiation profile of HSPCs in the developing zebrafish embryos and revealed that their differentiation into erythroid and myeloid lineages differs substantially both in time and location. In situ differentiation of HSPCs into definitive myeloid cells occurs as early as 2 dpf in VDA, the zebrafish AGM analogy, whereas differentiation into erythroid lineages is achieved only from 3-4 dpf onwards, when HSPCs have reached PBI, the zebrafish FL analogy. Hence, our findings suggest that developing HSPCs elicit different differentiation output as they home from one niche to another. During their transition, HSPCs first undergo myeloid differentiation in the VDA and later give rise to erythroid as well as myeloid lineages in the PBI. Recently, Kissa et al. have suggested that cells in the VDA with low level of *cd41*:eGFP expression are nascent zebrafish HSPCs (Kissa et al., 2008). Therefore, it would be of interest to track whether VDA localized definitive myeloid cells and PBI-localized definitive erythrocytes are derivatives of these *cd41*:eGFP^{low} cells, and, if so, to study the differentiation behavior of these cells with respect to cell division pattern as well as niche architecture.

We attribute selective emergence of definitive erythroid lineage in the PBI, at least in part, to the different micro-environment between the VDA and PBI, as HSPCs were unable to initiate definitive erythropoiesis when they were trapped in the VDA owing to circulation defects in the *sih* morphants. However, an ultimate demonstration for the impact of micro-environments on the differentiation output of HSPCs would be performing reciprocal transplantations with HSPCs isolated from these two sites. The success of such transplantation demands stringent isolation of HSPCs to highly purified fractions, which still awaits future technical advancement. At current stage, the molecular basis for the

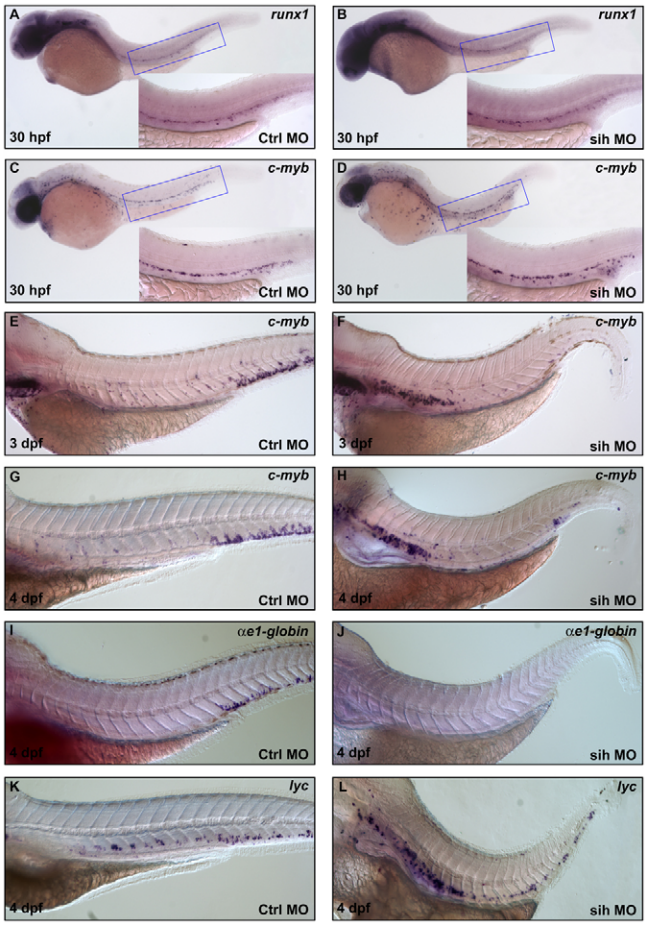

Fig. 6. Inhibition of HSPC migration from the VDA to PBI blocks their differentiation into erythroid but not myeloid lineages. (**A**,**B**) Whole-mount in situ hybridization of *runx1* expression in 30 hpf control MO injected *vlt*^{m651} embryos (A) and *sih* MO injected *vlt*^{m651} embryos (B). (**C-H**) Whole-mount in situ hybridization of *cmyb* expression in control MO-injected *vlt*^{m651} embryos at 30 hpf (C), 3 dpf (E) and 4 dpf (G); *sih* MO injected *vlt*^{m651} embryos at 30 hpf (D), 3 dpf (F) and 4 dpf (H). (**I**,**J**) Whole-mount in situ hybridization of αe1-globin expression in 4 dpf control MO injected *vlt*^{m651} embryos (I) and *sih* MO-injected *vlt*^{m651} embryos (J). (**K**,**L**) Whole-mount in situ hybridization of *lyc* expression in 4 dpf control MO-injected *vlt*^{m651} embryos (K) and *sih* MO-injected *vlt*^{m651} embryos (L). Insets are higher magnification (20×) views of the corresponding boxed regions (blue).

role of environmental cues in triggering the onset of definitive erythropoiesis in the PBI is not clear. It could be due to an inhibitory effect imposed by the VDA or the presence of erythroid inductive factors in the PBI. Although our data highlight the importance of environmental cues in determining the onset of definitive erythropoiesis, we could not underestimate the role of intrinsic program embedded in the developing HSPCs, which cooperates with environmental factors.

Bertrand et al. (Bertrand et al., 2007) recently reported the identification of committed erythromyeloid progenitors in the caudal part of precirculation embryos through which the first wave of definitive hematopoiesis initiates. VDA-originated HSPCs and committed erythromyeloid progenitors were mapped to anterior and posterior mesoderm, respectively, in the precirculation embryos, suggesting they originate independently of each other (Bertrand et al., 2007). In addition, unlike the transient existence of committed erythromyeloid progenitors, the number of which peaks at 30 hpf and declines from 40 hpf onwards (Bertrand et al., 2007), VDA-derived HSPCs probably represent self-renewing cells that will eventually migrate to kidney where they sustain definitive hematopoiesis throughout adulthood. Our study reveals that the differentiation of VDA-originated HSPCs is distinct from that of committed erythromyeloid progenitors. VDA-originated HSPCs elicit a niche-specific differentiation repertoire: they generate myeloid cells via in situ differentiation in the VDA but give rise to erythroid lineage later, after they home to the PBI. By contrast, the differentiation of committed erythromyeloid progenitors is always PBI restricted (Bertrand et al., 2007). Hence, differentiation from VDA originated HSPCs provides another source of myeloid and erythroid cells that is independent of those generated through committed erythromyeloid progenitors born in the caudal part. This additional wave of differentiation, which bridges between committed erythromyeloid progenitors initiated definitive hematopoiesis and kidney hematopoiesis, might reflect an evolutionary design to meet the need of rapidly developing fish embryo.

The in situ generation of definitive myeloid cells in the zebrafish AGM analogous region VDA is unexpected considering the currently held notion that, in mice, the AGM is not a site for hematopoietic stem cell differentiation (Godin et al., 1999; Cumano and Godin, 2007). However, our data are consistent with several published studies documenting the presence or enrichment of myeloid restricted progenitors in the mouse or chicken AGM (Cormier et al., 1986; Cormier and Dieter-Lievre, 1988; Ohmura et al., 1999; Palis et al., 1999). Among these, Palis et al. (Palis et al., 1999) have reported that compared with the rest of the embryo, AGM contained relatively high proportion of myeloid progenitors such as Mac-CFC and Mast-CFC at 30- to 43-somite pairs and 60-somite pairs, respectively. By contrast, definitive erythroid progenitors (BFU-E and CFU-E) do not display similar enrichment. Thus, it appears that autonomous generation of definitive myeloid but not erythroid cells in the AGM analogous region could be a common theme shared by all vertebrates. It is still unclear whether other lineages besides myeloid cells are produced in the AGM. The detection of *ikaros* expression, a presumptive lymphoid progenitor marker, in the VDA might suggest the co-existence of T cell progenitors in this region (Willett et al., 2001). However, further lineage tracing analysis is required to clarify this issue as *ikaros* is also expressed in the multipotent progenitors (Klug et al., 1998; Georgopoulos, 2002).

The nature of VDA-derived definitive myeloid cells and their physiological relevance remain to be elucidated. These myeloid cells may provide cytokines that are essential for the survival and proliferation of the neighboring HSPCs. A recent work by Robin et al. has revealed a crucial role for IL3 in promoting the proliferation or survival of hematopoietic stem cells in the AGM, although the identity of the IL3-producing cells was not determined in their study (Robin et al., 2006). Therefore, it is conceivable that myeloid cells derived from hematopoietic stem cells in the AGM represent such nurturing cells secreting paracrine growth factor for the stem cells. Alternatively, these earlier arising definitive myeloid cells may consist of macrophage populations, which are likely to be involved in promoting the maturation of definitive erythroid cells later in the PBI, as mammalian macrophages are reported to be indispensable for FL erythropoiesis (Kawane et al., 2001). This hypothesis is in accordance with our finding that VDA-derived myeloid cells are already detectable in the PBI as early as 2 dpf prior to the appearance of differentiated definitive erythrocytes in this site. Further investigations are required to clarify these issues.

We thank Jagman Chahal and Kevin Bishop for technical assistance. This work was supported in part by the Intramural Research Program of National Human Genome Research Institute, NIH (P.P.L.) and by grant from the Research Grants Council of Hong Kong to Z.L.W. (662808). Deposited in PMC for release after 12 months.

Supplementary material

Supplementary material for this article is available at http://dev.biologists.org/cgi/content/full/136/4/647/DC1

References

Akashi, K., Traver, D. and Weissman, I. L. (2000). A clonogenic common myeloid progenitor that gives rise to all myeloid lineages. *Nature* **404**, 193-197.

Bennett, C. M., Kanki, J. P., Rhodes, J., Liu, T. X., Paw, B. H., Kieran, M. W., Langenau, D. M., Delahaye-Brown, A., Zon, L. I., Fleming, M. D. et al. (2001). Myelopoiesis in the zebrafish, Danio rerio. *Blood* **98**, 643-651.

Bertrand, J. Y., Kim, A. D., Violette, E. P., Stachura, D. L., Cisson, J. L. and Traver, D. (2007). Definitive hematopoiesis initiates through a committed erythromyeloid progenitor in the zebrafish embryo. *Development* **134**, 4147-4156.

Brownlie, A., Hersey, C., Oates, A. C., Paw, B. H., Falick, A. M., Witkowska, H. E., Flint, J., Higgs, D., Jessen, J., Bahary, N. et al. (2003). Characterization of embryonic globin genes of the zebrafish. *Dev. Biol.* **255**, 48-61.

Burns, C. E., Traver, D., Mayhall, E., Shepard, J. L. and Zon, L. I. (2005). Hematopoietic stem cell fate is established by the Notch-Runx pathway. *Genes Dev.* **19**, 2331-2342.

Cormier, F. and Dieterlen-Lievre, F. (1988). The wall of the chick embryo aorta harbours M-CFC, G-CFC, GM-CFC and BFU-E. *Development* **102**, 279-285.

Cormier, F., De Paz, P. and Dieterlen-Lievre, F. (1986). *In vitro* detection of cells with monocytic potentiality in the wall of the chick embryo aorta. *Dev. Biol.* **118**,167-175.

Cumano, A., Ferraz, J. C., Klaine, M., Di Santo, J. P. and Godin, I. (2001). Intraembryonic, but not yolk sac hematopoietic precursors, isolated before circulation, provide long-term multilineage reconstitution. *Immunity* **15**, 477-485.

Cumano, A. and Godin, I. (2007). Ontogeny of the hematopoietic system. *Annu. Rev. Immunol.* **25**, 745-785.

Davidson, A. J. and Zon, L. I. (2004). The 'definitive' (and 'primitive') guide to zebrafish hematopoiesis. *Oncogene* **23**, 7233-7246.

de Jong, J. L. and Zon, L. I. (2005). Use of the Zebrafish to study primitive and definitive hematopoiesis. *Annu. Rev. Genet.* **39**, 481-501.

Gekas, C., Dieterlen-Lievre, F., Orkin, S. H. and Mikkola, H. K. (2005). The placenta is a niche for hematopoietic stem cells. *Dev. Cell* **8**, 365-375.

Georgopoulos, K. (2002). Haematopoietic cell-fate decisions, chromatin regulation and ikaros. *Nat. Rev. Immunol.* **2**, 162-174.

Gering, M. and Patient, R. (2005). Hedgehog signaling is required for adult blood stem cell formation in zebrafish embryos. *Dev. Cell* **8**, 389-400.

Godin, I., Garcia-Porrero, J. A., Dieterlen-Lievre, F. and Cumano, A. (1999). Stem cell emergence and hemopoietic activity are incompatible in mouse intraembryonic sites. *J. Exp. Med.* **190**, 43-52.

Herbomel, P., Thisse, B. and Thisse, C. (1999). Ontogeny and behaviour of early macrophages in the zebrafish embryo. *Development* **126**, 3735-3745.

Jin, H., Xu, J. and Wen, Z. L. (2007). Migratory path of definitive hematopoietic stem/progenitor cells during zebrafish development. *Blood* **109**, 5208-5214.

Jin, H., Xu, J., Qian, F., Du, L., Chee Yong Tan, C. Y., Lin, Z., Peng, J. R. and Wen, Z. L. (2006). The 5′ zebrafish scl promoter targets transcription to the brain, spinal cord, and hematopoietic and endothelial progenitors. *Dev. Dyn.* **235**, 60-67.

Kalev-Zylinska, M. L., Horsfield, J. A., Flores, M. V., Postlethwait, J. H., Vitas, M. R., Baas, A. M., Crosier, P. S. and Crosier, K. E. (2002). Runx1 is required for zebrafish blood and vessel development and expression of a human RUNX1-CBF2T1 transgene advances a model for studies of leukemogenesis. *Development* **129**, 2015-2030.

Kawane, K., Fukuyama, H., Kondoh, G., Takeda, J., Ohsawa, Y., Uchiyama, Y. and Nagata, S. (2001). Requirement of DNase II for definitive erythropoiesis in the mouse fetal liver. *Science* **292**, 1546-1549.

Keegan, B. R., Meyer, D. and Yelon, D. (2004). Organization of cardiac chamber progenitors in the zebrafish blastula. *Development* **131**, 3081-3091.

Kissa, K., Murayama, E., Zapata, A., Cortés, A., Perret, E., Machu, C. and Herbomel, P. (2008). Live imaging of emerging hematopoietic stem cells and early thymuscolonization. *Blood* **111**, 1147-1156.

Klug, C. A., Morrison, S. J., Masek, M., Hahm, K., Smale, S. T. and Weissman, I. L. (1998). Hematopoietic stem cells and lymphoid progenitors express different Ikaros isoforms, and Ikaros is localized to heterochromatin in immature lymphocytes. *Proc. Natl. Acad. Sci. USA* **95**, 657-662.

Kondo, M., Weissman, I. L. and Akashi, K. (1997). Identification of clonogenic common lymphoid progenitors in mouse bone marrow. *Cell* **91**, 661-672.

Kozlowski, D., Murakami, T., Ho, R. K. and Weinberg, E. S. (1997). Regional cell movement and tissue patterning in the zebrafish embryo revealed by fate mapping with caged fluorescein. *Biochem. Cell Biol.* **75**, 551-562.

Lawson, N. D. and Weinstein, B. M. (2002). *In vivo* imaging of embryonic vascular development using transgenic zebrafish. *Dev. Biol.* **248**, 307-318.

Lieschke, G. J., Oates, A. C., Paw, B. H., Thompson, M. A., Hall, N. E., Ward, A. C., Ho, R. K., Zon, L. I. and Layton, J. E. (2002). Zebrafish SPI-1 (PU.1) marks a site of myeloid development independent of primitive erythropoiesis: implications for axial patterning. *Dev. Biol.* **246**, 274-295.

Liu, F. and Wen, Z. L. (2002). Cloning and expression pattern of the lysozyme C gene in zebrafish. *Mech. Dev.* **113**, 69-72.

Lyons, S. E., Lawson, N. D., Lei, L., Bennett, P. E., Weinstein, B. M. and Liu, P. P. (2002). A nonsense mutation in zebrafish gata1 causes the bloodless phenotype in vlad tepes. *Proc. Natl. Acad. Sci. USA* **99**, 5454-5459.

Mebius, R. E., Miyamoto, T., Christensen, J., Domen, J., Cupedo, T., Weissman, I. L. and Akashi, K. (2001). The fetal liver counterpart of adult common lymphoid progenitors gives rise to all lymphoid lineages, CD45+CD4+CD3- cells, as well as macrophages. *J. Immunol.* **166**, 6593-6601.

Medvinsky, A. and Dzierzak, E. (1996). Definitive hematopoiesis is autonomously initiated by the AGM region. *Cell* **86**, 897-906.

Melby, A. E., Warga, R. M. and Kimmel, C. B. (1996). Specification of cell fates at the dorsal margin of the zebrafish gastrula. *Development* **122**, 2225-2237.

Mikkola, H. K. and Orkin, S. H. (2006). The journey of developing hematopoietic stem cells. *Development* **133**, 3733-3744.

Muller, A. M., Medvinsky, A., Strouboulis, J., Grosveld, F. and Dzierzak, E. (1994). Development of hematopoietic stem cell activity in the mouse embryo. *Immunity* **1**, 291-301.

Murayama, E., Kissa, K., Zapata, A., Mordelet, E., Briolat, V., Lin, H. F., Handin, R. I. and Herbomel, P. (2006). Tracing hematopoietic precursor migration to successive hematopoietic organs during zebrafish development. *Immunity* **25**, 963-975.

Ohmura, K., Kawamoto, H., Fujimoto, S., Ozaki, S., Nakao, K. and Katsura, Y. (1999). Emergence of T, B, and myeloid lineage-committed as well as multipotent hemopoietic progenitors in the aorta-gonad-mesonephros region of day 10 fetuses of the mouse. *J. Immunol.* **163**, 4788-4795.

Okuda, T., van Deursen, J., Hiebert, S. W., Grosveld, G. and Downing, J. (1996). AML1, the target of multiple chromosomal translocations in human leukemia, is essential for normal fetal liver hematopoiesis. *Cell* **84**, 321-330.

Ottersbach, K. and Dzierzak, E. (2005). The murine placenta contains hematopoietic stem cells within the vascular labyrinth region. *Dev. Cell* **8**, 377-387.

Palis, J., Robertson, S., Kennedy, M., Wall, C. and Keller, G. (1999). Development of erythroid and myeloid progenitors in the yolk sac and embryo proper of the mouse. *Development* **126**, 5073-5084.

Qian, F., Zhen, F. H., Xu, J., Huang, M., Li, W. and Wen, Z. L. (2007). Distinct functions for different scl isoforms in zebrafish primitive and definitive hematopoiesis. *PLoS Biol.* **5**, 1110-1119.

Robin, C., Ottersbach, K., Durand, C., Peeters, M., Vanes, L., Tybulewicz, V. and Dzierzak, E. (2006). An unexpected role for IL-3 in the embryonic development of hematopoietic stem cells. *Dev. Cell* **11**, 171-180.

Samokhvalov, I., Samokhvalova, M. N. I. and Nishikawa, S. (2007). Cell tracing shows the contribution of the yolk sac to adult haematopoiesis. *Nature* **446**, 1056-1061.

Sehnert, A. J., Hug, A., Weinstein, B. M., Walker, C., Fishman, M. C. and Stainier, D. Y. (2002). Cardiac troponin T is essential in sarcomere assembly and cardiac contractility. *Nat. Genet.* **31**, 106-110.

Serbedzija, G. N., Chen, J. N. and Fishman, M. C. (1998). Regulation in the heart field of zebrafish. *Development* **125**, 1095-1101.

Sood, R., English, M. A., Jones, M., Mullikin, J., Wang, D. M., Anderson, M., Wu, D., Chandrasekharappa, S. C., Yu, J., Zhang, J. et al. (2006). Methods for reverse genetic screening in zebrafish by resequencing and TILLING. *Methods* **39**, 220-227.

Thompson, M. A., Ransom, D. G., Pratt, S. J., MacLennan, H., Kieran, M. W., Detrich, H. W., 3rd, Vail, B., Huber, T. L., Paw, B., Brownlie, A. J. et al. (1998). The cloche and spadetail genes differentially affect hematopoiesis and vasculogenesis. *Dev. Biol.* **197**, 248-269.

Traver, D., Miyamoto, T., Christensen, J., Iwasaki-Arai, J., Akashi, K. and Weissman, I. L. (2001). Fetal liver myelopoiesis occurs through distinct, prospectively isolatable progenitor subsets. *Blood* **98**, 627-635.

Traver, D., Paw, B. H., Poss, K. D., Penberthy, W. T., Lin, S. and Zon, L. I. (2003). Transplantation and *in vivo* imaging of multilineage engraftment in zebrafish bloodless mutants. *Nat. Immunol.* **4**, 1238-1246.

Vincent, J. P. and O'Farrell, P. H. (1992). The state of *engrailed* expression is not clonally transmitted during early Drosophila development. *Cell* **68**, 923-931.

Westerfield, M. (1995). *The Zebrafish Book: A Guide for the Laboratory Use of Zebrafish* (Danio rerio). 3rd edn. Eugene, OR: University of Oregon Press.

Willett, C. E., Kawasaki, H., Amemiya, C. T., Lin, S. and Steiner, L. A. (2001). Ikaros expression as a marker for lymphoid progenitors during zebrafish development. *Dev. Dyn.* **222**, 694-698.